Active Site Expansion of Superoxide reductase (SOR) Induced by X-Rays Photoreduction

Virgile Adam[ab], Antoine Royant[b], Vincent Nivière[c], Fernando P. Molina-Heredia[c] & Dominique Bourgeois[ab]

[a] European Synchrotron Radiation Facility (ESRF), Experiment Division, 6 rue Jules Horowitz, BP 220, 38043 Grenoble Cedex, France
[b] Institut de Biologie Structurale (IBS), Laboratoire de Cristallographie et Cristallogénese des Protéines (LCCP), UMR 9015, 41 avenue Jules Horowitz, 38027 Grenoble Cedex 1, France
[c] Comissariat à l'Energie Atomique (CEA), Chimie Biochimie des Centres Redox Biologiques (CBCRB), 17 avenue des Martyrs, 38054 Grenoble, Cedex 9, France

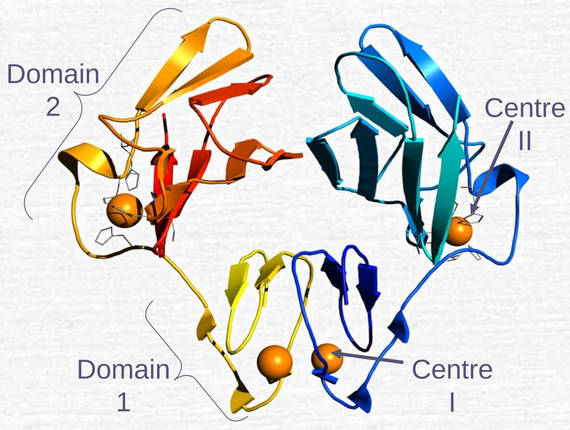

Fig. 1 Three-dimensional structure of *D. baarsii* SOR

1) What is a superoxide reductase?

Superoxide reductase (SOR) is a metallic-enzyme eliminating the superoxide anion:

$$O_2^{-\cdot} + 2H^+ + SOR(Fe^{2+}) \rightarrow H_2O_2 + SOR(Fe^{3+})$$

As it is found in sulphure-reducing and microaerophilic bacteria, the advantage of SOR compared to superoxide dismutase (SOD) is that there is no oxygen release in the cell. However, the reaction catalyzed by SOR is formally the same as the second half reaction catalyzed by SOD.
Desulfoarculus baarsii SOR has two iron centers with the following redox potentials: +4 mV for centre I, whose physiological role remains unclear, and +240 mV for centre II, where $O_2^{-\cdot}$ binds. The enzyme is naturally found in a hemi-reduced form, with centre I oxydized and centre II reduced. Center II is insensitive to oxygen, but can be oxidized in solution with powerful oxidizers like hexachloroiridate, hexacyanoferrate and of course, the substrate, superoxide.

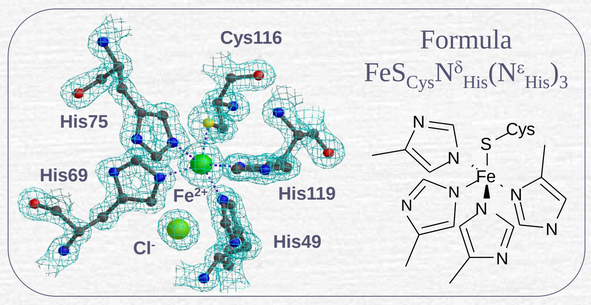

Fig.2 Detail of the SOR active site (center II) and of a stabilized chloride atom close to the iron

2) The structure of superoxide reductase

The structure of SOR (fig.1) shows a globular homodimeric protein. Each monomer is composed of two domains, each holding an iron center. In center I, the iron atom is surrounded by four cysteines in a square-pyramidal conformation, a commonly found coordination pattern. In center II (fig.2), which is the active site, the iron atom is coordinated by four histidines and a cysteine, a quite unusual coordination pattern.
In the reduced state, the sixth coordination, where superoxide is expected to bind, is vacant. The substrate binding pocket is a strong anion attractor and we have noticed the presence of a chloride atom (present the crystallization medium) stabilized at 4Å from the iron by a network of water molecules.
The mutant we are using (Glu47Ala) is thought to stabilize a (hydro) peroxo intermediate along the reaction pathway. It is therefore of interest to obtain the structure of this oxidized SOR mutant.
By optimizing crystallization conditions (fig.3), we could solve the structure of the reduced form at 1.15Å.

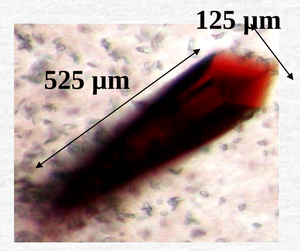

Fig.3 SOR crystal in its hemi-reduced form (red)

3) Structure of the oxidized form

We could co-crystallize SOR with hexacyanoferrateIII also known as ferricyanide ($Fe(CN_6)^{4-}$). Unexpectedly, the structure clearly shows a ferricyanide strongly bound to the center II iron through a bent cyanide group (fig.4) due to charge attraction from the active site and a good fitness of shape of ferricyanide.
Biochemical studies lead on both the mutant and wild-type protein have shown that a strong decrease of SOR activity is induced by this complexation. This inhibition is however incomplete despite of the observed nearly perfect plugging (fig.5). We are still working on this precise point.

Also unexpectedly, the excess of ferricyanide added to crystallization drops resulted in the loss of 65% of the center I iron atoms. Therefore we find partial occupation in this center for cysteines forming disulphide bridges.
This loss of center I iron atoms, is fortunate as it resulted in the possibility to observe the 650 nm absorption band of center II much more easily since center I signal normally overwhelms the signal of the oxidized active site. We could thus verify that in crystals of the complex, before X-ray data collection, the center II iron was oxidized.

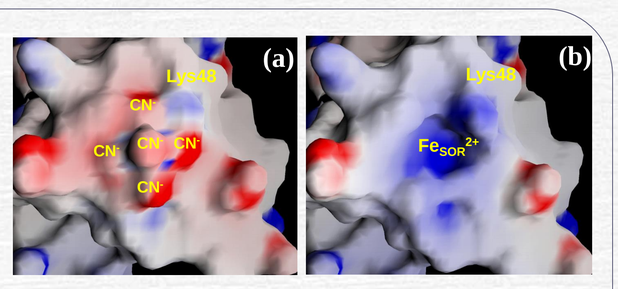

Fig.4 GRASP Electrostatic surface potential of SOR with (a) and without (b) ferrocyanide bound, contoured from -25 (red) to +25 (blue) kTe^{-1}.

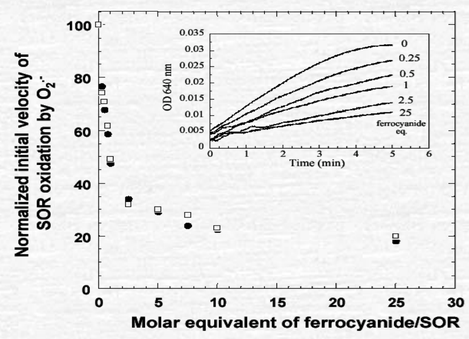

Fig.5 Initial velocity of the oxidation of the SOR (wt and E47A mutant) centre II by superoxide in presence of $Fe(CN)_6$

4) Radiation damage

Data collection on SOR-$Fe(CN)_6$ crystals (grey-green), resulted in clear radiation damage induced by X-rays, as assessed by visual inspection (fig.6). Following time-dependence on the high brilliance beamline ID14-4 revealed that rapid photoreduction of both centers I and II occurred during data collection.

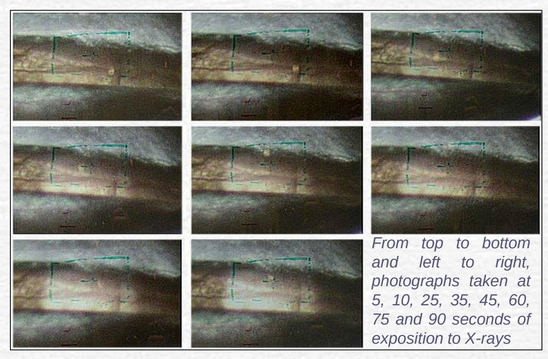

From top to bottom and left to right, photographs taken at 5, 10, 25, 35, 45, 60, 75 and 90 seconds of exposition to X-rays

Fig.6 Development of radiation damage on a needle-shaped crystal of complexed SOR

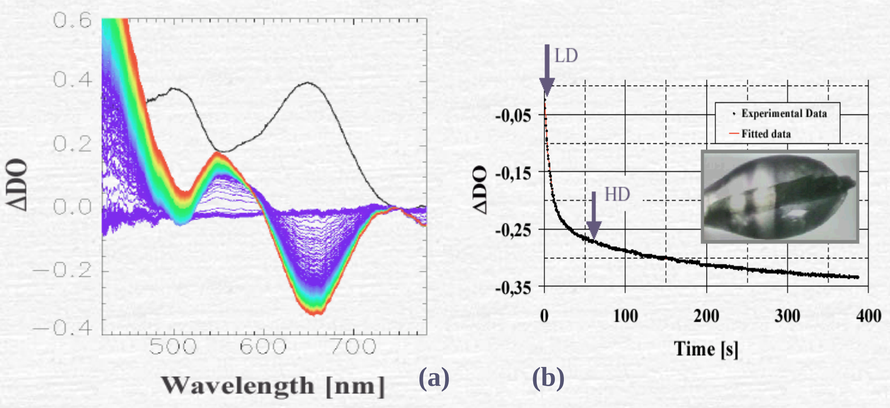

Fig.7 (a) Online difference absorbance spectra recorded on SOR co-crystallized with $Fe(CN)_6$ collected during a 400 sec X-ray exposure [initial spectrum : black, set as baseline] and (b) decay of the ~ 650 nm absorption band

5) Composite datasets

A real-time absorbance measurement in the crystal during X-ray exposure (fig. 7a) showed a very fast reduction of the 650 nm band ($t_{1/2}$ = 10 seconds) specific of the oxidized active iron (fig. 7b). In order to obtain a "low-dose" oxidized structure and a "high-dose" reduced structure, we collected several partial data sets with an attenuated beam on the same long needle-shaped crystal, and recombined them to form two "composite" data sets (fig.8). The "low-dose" dataset corresponded to 6 seconds of exposition under the attenuated beam and the "high-dose" dataset corresponded to 80 seconds of exposition under the non-attenuated beam (fig.9).

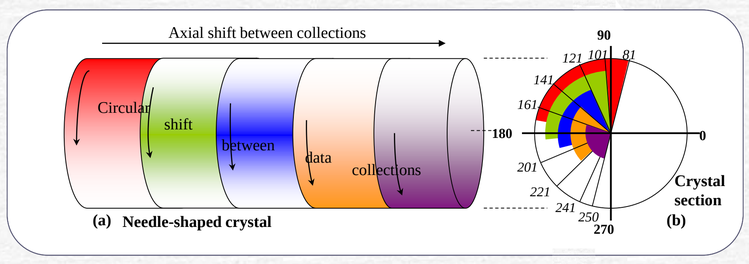

Fig.8 Representation of the method applied to collect subsets used to build the composite datasets

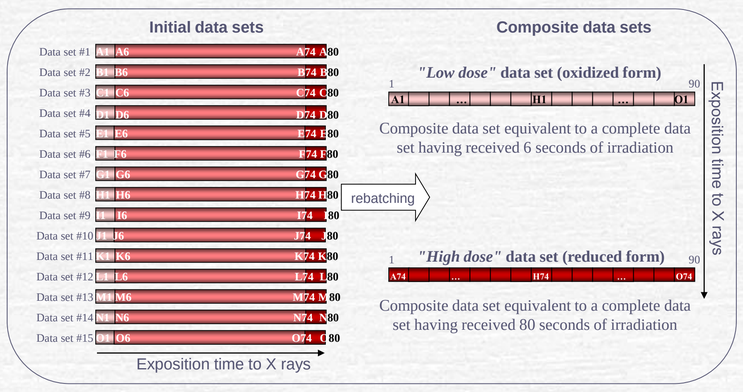

Fig.9 Rebatching strategy of the partial data sets to build composite datasets independent of time exposition to X-rays

6) Fourier difference maps

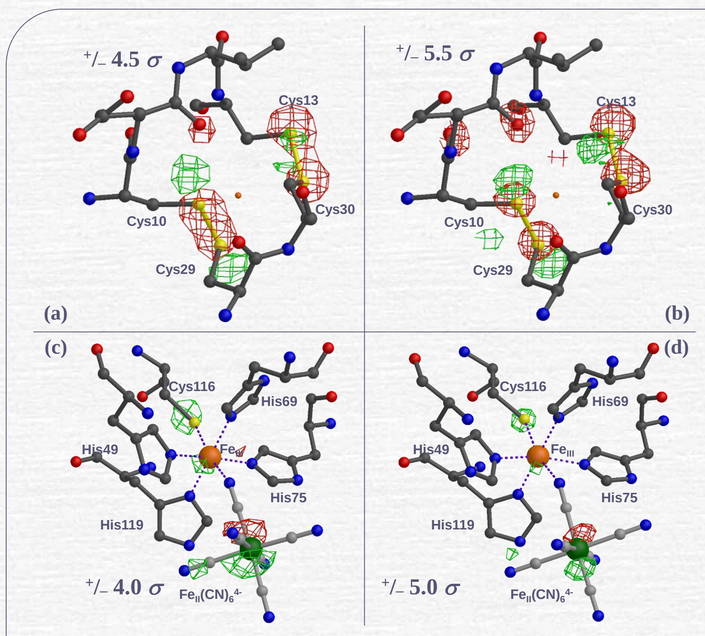

Fig.10 Difference maps of the (reduced – oxidized) structures for center I (a,c) and center II (b,d) respectively with observed and calculated structure factors

The $(F_{obs,reduced} - F_{obs,oxidized})$ difference maps (fig.10a,c) between the oxidized and reduced models of the complex with $Fe(CN)_6$ (solved at 1.7Å) are consistent with X-ray induced reduction of the molecule.
We have also calculated $(F_{calc,reduced} - F_{calc,oxidized})e^{i.\varphi calc,oxidized}$ difference maps (fig.10b,d) which show the same peaks and prove that no bias was introduced during the refinement.
As an internal control, a clear reduction of two disulphide bridges formed by the cysteines of center I can be observed (fig.10a,b). Modelization of these cysteines turned out to be much easier in these structures than in a dose-dependant (standard) data set where mixed conformations exist.
In center II (fig.10c,d), a slight but significant coordination expansion (more than 5%) is observed. All atoms around the iron moved slightly away. All these results are consistent with a decrease of the iron charge by one electron, thereby reducing the electrostatic attraction of the coordinating ligands.

7) Conclusion

The described SOR crystal structure in complex with hexacyanoferrate is the first protein structure solved with this compound.
Our results show that it is possible to follow in real time by microspectrophotometry the reduction of a metalloenzyme by a synchrotron X-ray beam. The technique of composite datasets allows to observe the associated subtle coordination expansion with unprecedented accuracy in a protein.
Preliminary biochemical studies show that ferrocyanide could be a partial inhibitor of the enzyme or a scavenger of superoxide, and may thus have a significant physiological relevance.

References / acknowledgements

[1] Jenney, F. *et al.* (1999) Science **286**(5438): 306-309
[2] Lombard, M. *et al.* (2000) J. of Biol. Chem. **275**(35): 27021-27026
[3] Mathé, C. *et al.* (2002) J. Am. Chem. Soc. **124**(18): 4966-4967
[4] Berglund, G.I. *et al.* (2002) Nature **417**: 463-468.

IBS Institut de Biologie Structurale (Grenoble)